# III. HIGHLIGHTS ON THE NEBULAE

C.Y. ZHANG

Y. TERZIAN
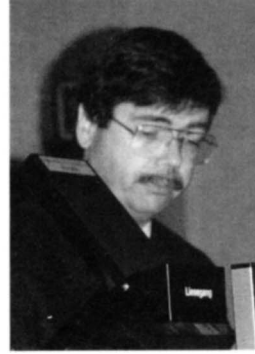
G. FERLAND

B. BALICK

Y.-H. CHU

P.J. HUGGINS

A.G.G.M. TIELENS
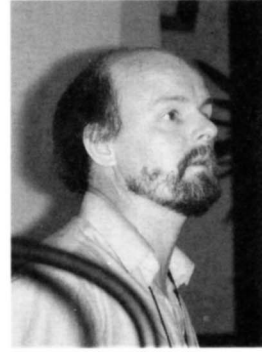
M.J. BARLOW

# ENERGY DISTRIBUTION OF PLANETARY NEBULAE (UV TO RADIO)

C.Y. ZHANG

*Department of Astronomy*
*The University of Texas at Austin*
*Austin, TX 78712*

**Abstract.** The past decade has seen significant progress in our understanding of spectral energy distribution of planetary nebulae over the entire wavelength range from UV to radio. In this review we show the detailed breakdown of the energy budget for a planetary nebula as a system of the three components, i.e., the central star, the gaseous nebula and the dust shell. This picture of the energy distribution is further discussed in the context of planetary nebula evolution.

## 1. Introduction

The major obstacle to fully comprehend the energetics in planetary nebulae (PN) had been the difficulty of obtaining the completely continuous spectrum, which has a comparable energy output in the infrared, ultraviolet, and optical wavelength ranges. Dramatic progress has been made in our understanding of spectral energy distribution (SED) of PN since the last decade. It largely results from our access to instruments covering a vastly broad wavelength range. The modern techniques and instruments, including the VLA, IRAS, through IUE to Einstein, EXOSAT and ROSAT, have allowed extension of the wavelength coverage from the conventional optical, to radio, infrared, UV, and even X-ray.

## 2. Components of a Planetary Nebula System

A PN system is made up of three major components: a central star, an ionized gas nebula, and a dust shell. These three major components can be further divided to include the ionized stellar wind from the star, a high temperature "bubble" formed by the interaction of this wind with the nebula and a neutral gas envelope if the nebula is ionization-bounded (Kwok 1982). The spectrum of the central star can be approximated by a blackbody of temperature 30,000 to 200,000 K. There can be departures from the Planck spectrum (especially in the UV) due to transfer effects in the stellar atmospheres. The ionized nebula is dominated by bound-free, free-free, and two-photon continuum emissions, and recombination and collisionally-excited line emissions. The dust envelope is responsible for thermal continuum emission at a dust temperature of about 100 K.

## 3. Energy Distribution of Planetary Nebulae

It is only recently that a significant number of PN have been observed over a wide spectral range from UV to radio for their energetics to be studied in a systematic manner. If a PN is ionization-bounded, the present wavelength coverage from the radio to 0.1 $\mu$m probably contains most of the energy emitted. For density-bounded nebulae, there could be flux missing in the far- ultraviolet.

99

## 3.1. PROGRESS IN OBSERVATIONS

UV observations have played an important role in our understanding of energy distribution of PN. It is crucial to observe them in this wavelength regime, where the energy distribution becomes more sensitive to the temperature of the central star, compared to that in the optical. The IUE observations of more than 200 PN have demonstrated that (1) the two-photon emission is one of the essential ingredients in nebular continuum (Pottasch 1984), and (2) the UV spectrum is vital for studying properties of stellar energy distribution (Kaler and Feibelman 1985, Heap and Augensen 1987, Bianchi et al. 1989).

In an attempt to determine accurate stellar magnitudes, narrow or intermediate band photometric data of PN have been accumulated, particularly through the work done by Webster (1988), Kaler (1976a, 1978), Kohoutek and Martin (1981; KM), and Shaw and Kaler (1985, 1989; SK). The above work was usually aimed at determination of the central star B and V magnitudes. For a review on the various techniques in this regard see Kaler (1989). SK have carried out narrow-band continuum and emission-line photometry for 145 southern hemisphere PN. They have obtained B and V magnitudes for 120 central stars after subtracting nebular continuum from the total flux recorded. The continuum fluxes at 3226, 3546, 4225, 5306, 6865, and 7901 $\mathring{A}$ were measured by KM using narrow-band photometry. This set of data are extremely useful in that the Balmer jump is clearly revealed in emission for their sample PN. The requirement, that any model to fit the SED of these PN must be able to fit the Balmer jump, gives very tight constraints on determinations of relative contributions from the nebula and the central star to the continuum in the wavelength range from UV to optical. It is particularly interesting to see the magnitudes of the central star and the global nebular continuum were derived simultaneously for 11 PN, based on the nebula-subtraction method using CCD imagery (Jacoby and Kaler 1989).

An unparalleled, extensive spectroscopic survey of about 1000 PN have been conducted by Acker and Stenholm (1987). This provides a unique means to study SED for a large sample of PN. Spectroscopic measurements of the continuum are free of contamination from line emission. In deriving stellar magnitudes, Tylenda et al. (1991a) have measured the continuum levels at 4 wavelength points. Bearing in mind that these authors were interested in stellar B and V magnitudes, they gave the ratios of stellar to total continuum at three wavelengths (4340, 4860, and 6560 $\mathring{A}$) and the stellar flux at 4860 $\mathring{A}$. In Tylenda et al. (1989), the stellar fluxes at both 4860 and 6560 $\mathring{A}$ were given. Since the aperture used was 4", the total continuum flux can be obtained for a nebula with a size less than 4". Kaler et al. (1990) presented spectrophotometry of 75 large PN and derived B and V magnitudes for 17 central stars of them. The total continuum including nebular and stellar parts is not available from their paper. Kaler et al. (1991) have obtained the continuum fluxes at 1300, 1500, 1750, 4000, 4310, and 5480 $\mathring{A}$ for PB6.

Near-infrared (near-ir) photometry has been obtained by several groups (White-lock 1985; Kwok et al. 1986; van der Veen et al. 1989; Preite-Martinez and Persi 1989). Some PN are identified in a near-ir survey of PN candidates selected from their IRAS colors (Manchado et al. 1989; Garcia-Lario et al. 1990). Very recently,

Rudy et al. (1991a, b) have obtained the spectra of NGC 6572 and BD+303639 between 0.5 to 1.3 $\mu$m, and analyzed the continuum of them. Zhang and Kwok (1992) published the spectra of IC418 and IC5117 from 0.5 to 1.75 $\mu$m and modeled the continuum. These studies show that the near-ir is an important wavelength regime yet to be more extensively explored. Besides the rich emission lines, the stellar emission, bound-free, free-free emission, sometimes hot dust thermal emission, and possible dust features all contribute to the continuum in the near-ir.

IRAS has provided not only the most complete far-infrared (far-ir) photometric measurements (IRAS PSC), but also the very extensive far-ir spectroscopic data for PN (IRAS LRS). Volk and Cohen (1990) have extracted 170 spectra of PN from the LRS raw database. Zhang and Kwok (1990) have made a quantitative chemical analysis of solid material in 13 young PN, using the IRAS LRS spectra. They found that six of them show both oxygen- and carbon- rich dust features, and the silicate 18 $\mu$m feature is prominent in a number of young PN.

Strong line emission is one of the most prominent characteristics of PN, and a significant amount of energy is emitted in the atomic and even molecular lines. In the optical, the classical sources of these line data come from Kaler (1976b), Aller and Czyzak (1979, 1983), KM, Torres-Peimbert and Peimbert (1977) and others. Acker et al. (1989a) and SK provide the most recent results of line fluxes for a large number of PN. Line flux measurements are extended to the UV (Marionni and Harrington 1981; Boggess et al. 1981; Aller and Keyes 1981) and to far-ir (Pottasch et al. 1986; Zhang and Kwok 1990).

The absolute flux in the H$\beta$ line is one of the most important physical parameters for a study of PN, since all the line fluxes are scaled to H$\beta$. The most comprehensive measurements of the absolute H$beta$ flux is given by Acker et al. (1989a, b). This important quantity is now available for 880 PN owing to the most extensive spectroscopic survey done by the Acker's group.

Despite the impressive progress, the data of emission line fluxes cannot be complete, since different authors concentrated on limited wavelength ranges. In particular, in the near- and far-ir, emission lines have not been explored as thoroughly as in the optical.

Early in the 60's and 70's, single dish radio continuum measurements had established the spectral distribution of PN in the radio (for a review, see, Terzian 1991). Beginning from the 70's, high resolution mapping of PN with the VLA (Aaquist and Kwok 1990; Zijlstra et al. 1989; Ratag et al. 1990) have resulted in radio images, accurate flux densities, and angular sizes for 402 PN.

Kreysing et al. (these proceedings) reported the results from the ROSAT survey and found extended X-ray emission from six PN. The X-ray spectral distribution has ruled out the central as a source of the X-ray emission.

## 3.2. PLANETARY NEBULAE IN SYSTEMS AT KNOWN DISTANCES

Studies of PN in systems for which the distances can be determined are very important to our understanding of the intrinsic properties and evolution of PN. Knowledge of energy distribution of PN in the galactic bulge (GBPN) has significantly increased since the extensive spectroscopic data are now available for more than

300 GBPN (Acker et al. 1991; Tylenda et al. 1991b; Stasinska et al. 1991; Stasinska these proceedings). The B and V magnitudes of their central stars are obtained from the continuum in the spectra. This has led to determinations of the central star temperature and luminosity (Tylenda et al. 1991b). Progress has been also made in studies of PN in Magellanic Clouds (MCPN). Meatheringham and Dopita (1991) presented detailed spectroscopy in the optical for a sample of 41 MCPN and obtained central star magnitudes from the continuum. Other spectroscopic surveys of MCPN include those carried out by Monk et al. (1988) and Boroson and Leibert (1989).

One of the advantages to study the GBPN, and in particular, the MCPN, is that they are usually small so that the flux integrated over the entire nebula can be completely recorded. However, the disadvantage is that it is hard to measure them in the far-ir, where a significant fraction of the power is emitted. Contamination by foreground objects might be a problem for GBPN studies.

## 3.3. OBSERVED ENERGY DISTRIBUTION

Zhang and Kwok (1991) compiled observations of 66 compact PN in the whole wavelength range, and made a model fitting to the observed SED from 0.1 to about 100 $\mu$m (Fig. 1). Almost all nebulae show strong emissions over the three decades of wavelengths. The Balmer jump in emission can clearly seen (KM). To illustrate a wealth of emission lines, we plotted vertical lines at the line center wavelengths in Fig. 1. In contrast to the richness in lines in the optical, no lines are indicated in the near-ir, due to lack of the near-ir spectrum. The observed SED exhibits a double-peaked shape with a cut-off at about 0.1 $\mu$m, beyond which little is known.

## 4. Model of Energy Distribution

It is necessary to model the observed SED, in order to obtain a detailed breakdown of the energy coming from the different components of the system, because the contributions from a specific component cannot usually be directly measures in the observed spectrum.

## 4.1. MODEL COMPONENTS

The observed monochromatic flux is fitted by a following function:

$$F_\lambda = F_\lambda(star) + F_\lambda(gas) + F_\lambda(dust) \tag{1}$$

where $F_\lambda(star)$, $F_{lambda}(gas)$, and $F_{lambda}(dust)$ are the stellar photospheric continuum flux, the nebular gaseous continuum emission flux, and the nebular dust thermal emission flux, respectively. The nebular bound-free and free-free emission from HI, HeI and HeII, and hydrogen two-photon emission are taken into account in the effective gaseous continuum emission coefficient ($\gamma_{eff}$). Calculations of $\gamma_{eff}$ as a function of y1, y2, $T_e$ and $n_e$ are based on the formalism of Brown and Mathews (1970), with an extension to 1000 $\mathring{A}$ on the short wavelength side and to 20 $\mu$m on the long wavelength side. Four quantities, the angular radius of the star ($\theta_*$), the

central star temperature ($T_*$), the dust optical depth, and the dust temperature ($T_d$), in this model are used as free parameters to be optimized.

## 4.2. RESULTS

The individual model components are shown along with the synthesized model continuum in Fig. 1. The stellar flux points in the optical wavelength range determined by Shaw and Kaler (1989) and Tylenda et al. (1989) are given for comparison with the best- fit model stellar components. They are in good agreement with the model in most cases. Extrapolation from optically thin radio continuum flux densities is shown as a dashed line in Fig. 1. Dotted lines represent the bound-free, free-free, and two-photon emission from the ionized gas. A Planck function with a single temperature can fit the IRAS points well, indicating that the emitting dust is located near the nebular shell and is not distributed over a large volume as in the case of HII regions.

## 4.3. PHYSICAL PARAMETERS

Four parameters are derived from the model fitting: the temperature ($T_d$) and optical depth ($\tau$) of the dust component, and the angular size ($\theta_*$) and temperature ($T_*$) of the central star.

   The derived central star temperatures are in good agreement with the energy-balance temperature ($T_{EB}$) and the hydrogen Zanstra temperature [$T_Z(H)$]. The agreement with $T_Z(HeII)$ and the previously determined color temperature ($T_c$) is not particularly good. Three nebulae in the sample are in common with those of Mendez et al. (1988; MKHHG), who determined the effective temperatures spectroscopically. These are IC2448, He2-138, and M1-26, which have our $T_* = 80,000$, 33,100 and 33,100 K and the effective temperatures of $T_{eff} = 65,000$, 27,000, and 33,000 K from MKHHG respectively. The agreement between them is good in general, except for IC2448. It is not clear what causes this discrepancy (Zhang and Kwok 1991).

   The total fluxes for the three model components can be obtained by integrating the individual component over wavelengths. These are the non-ionizing stellar flux ($F_*$), nebular flux due to bound-free, free-free, and two-photon emission ($F_n$), and the far-ir flux ($F_{IR}$). The total line flux ($F_l$) is a summation of all emission line fluxes. To obtain the total observed flux from all the components, one should correct for the part of energy that is absorbed from the stellar non-ionizing radiation and converted into the far-ir radiation by dust. This correction will be important when the infrared excess (IRE) is larger than unity and at the same time the central star temperature is lower than 40,000 K. The amount of correction also depends on the optical properties of dust grains. Assuming that the central star radiates like a blackbody and the dust absorption coefficient varies with wavelength as a power law with an index of -1, one can estimate the fraction of the energy absorbed in UV out of that absorbed in the entire wavelength range, y, which is a function of $T_*$. Only the amount of energy surpassing the $Ly\alpha$ flux, i.e., ($F_{IR} - F_{Ly\alpha}$), where $F_{IR}$ and $F_{Ly\alpha}$ are in units of $F_{H\beta}$, should be corrected for this effect, so that
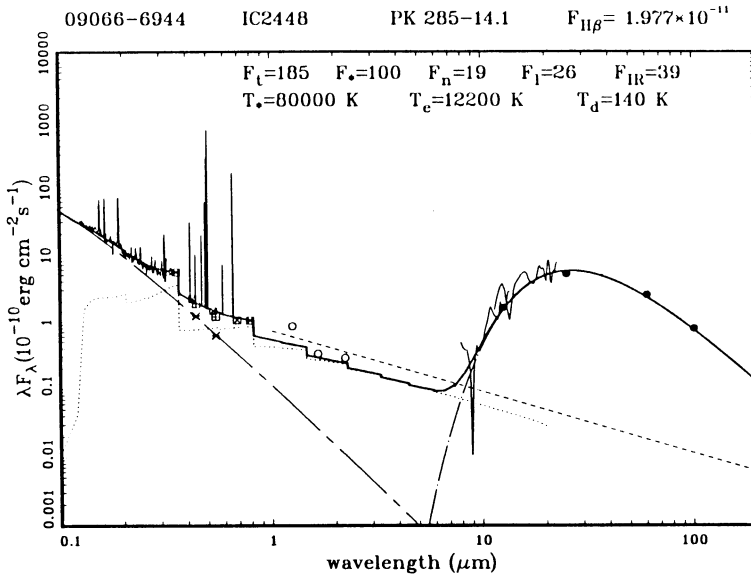
Fig. 1. The energy distribution of IC2448. Vertical lines illustrate emission lines. Model curves for the stellar, nebular, and dust components are shown as chain-dashed, dotted, and chain-dotted lines respectively. Thick solid lines show the synthesized energy distribution. Dashed lines indicate the level of free-free emission extrapolated from the optically thin radio continuum flux densities. Thin lines are the IUE and IRAS LRS spectra. Data points are from KM, SK, and Whitelock (1985)

the amount of energy absorbed by dust from the non-ionizing stellar radiation is now $F_c = (F_{IR} - F_{Ly\alpha}) \times (1 - y)$. Thus the total observed flux from a nebula is $F_t = (F_* - F_c) + F_n + F_l + F_{IR}$. It turns out that $F_c$ is less than about a few percent of $F_t$ for the majority sample nebulae, except for BD+303639 (30%) and M1-11 (20%).

We find that a significant fraction (38%) of the total observed flux is from the dust component. In the near-ir, almost all contribution to the observed fluxes are due to the nebular bound-free and free-free emission. In the visible, the star and nebula contribute approximately equally, depending on the central star temperature. In the UV, contribution from the central star often exceeds that of the nebular component.

## 4.4. OPTICAL THICKNESS

Supposing that the total flux integrating the Planck function at $T_*$ over the entire wavelength range (FBB) could represent the "true" total flux emitted by the central star, one can define an optical "thinness", $Q = (F_{BB} - F_t)/F_t$. It is found that the majority of the sample compact PN are optically thick to ionizing radiation. If $-0.4 < Q < 0.4$, the difference between $F_{BB}$ and $F_t$ can probably be attributed to the uncertainties in the fitting. A few PN with $Q > 0.6$ are likely to be optically

thin. Seven PN have $Q < -0.6$, which is likely to be caused by (1) an excess in the far-UV of the stellar spectrum; or (2) the nebula being not spherically symmetric. For three nebulae in common with the sample of MKHHG we found that M1-26 and He2-138 are optically thick, while IC2448 is optically thin. Mendez et al. (1992) found that the fraction of stellar ionizing luminosity absorbed by the nebula for these three PN are 0.7, 0.96, and 0.23 respectively, which is consistent with our results.

While Mendez et al. (1992) concluded that the majority of their nebulae are optically thin, our sample seems to contain more optically thick ones. This is likely due to selection effects. We have selected compact nebulae, of which the size is sufficiently small to ensure that all the nebular emission is properly registered in the observations. MKHHG's sample contains the brightest central stars to allow for the analysis of absorption line profiles. It is conceivable that as a PN system evolves and a nebula expands with time, the nebula may evolve from optically thick to optically thin. It is, therefore, very probable that our sample contains mostly young PN.

For the 27 objects in our sample with $T_Z(H) < T_Z(HeII)$, only 5 have $Q > +0.5$, implying optical thinness to the ionizing radiation. The rest of them show mostly negative $Q$ values and $-0.15 < Q < 0.1$. These nebulae are unlikely to be far from optically thick stage. We suggest that for these nebulae, the Zanstra temperature discrepancy and Q nearly zero are indications that the photospheres of many of these central stars have an UV excess relative to a blackbody beyond the He+ ionization threshold due to a lower-than-solar helium abundance in the atmospheres (Henry and Shipman 1986; Clegg and Middlemass 1987; Husfeld et al. 1984).

## 4.5. RATIOS OF THE TOTAL FLUX OVER $H\beta$ AND OVER THE IN-FRARED FLUX

We find that the ratio of the total flux over the $H\beta$ flux has a median of 160, consistent with the earlier result of Gathier and Pottasch (1989) for a sample of more extended nebulae. However, the ratio has a wide range from 90 to 620. It varies with $T_*$ and the dust mean UV optical depth. The curves of $L_* / L_{H\beta}$ as a function of $T_*$ for an ionization-bounded nebula with $\tau_{UV} = 0.0, 0.5, 1.0, 1.5, and 2.0$ are plotted in Fig. 2 along with the data points.

Most nebulae with moderate $Q$ values which are encompassed by the theoretical curves are likely to be ionization-bounded and enriched with dust grains. The reason for many of them to be locate above the $\tau_{UV} = 0$ curve lies in the fact that they are young nebulae with strong dust emission. However, two nebulae with higher $Q$ values, IC2149 and IC2448, are probably density-bounded.

In contrast to the above nebulae with large positive $Q$, six nebulae with large negative $Q$ values are located well below the $\tau - UV = 0$ curve. It cannot be explained by any effects of dust grains or optical thickness of the nebulae. It appears that there may be an excess in the far-UV portions of the emergent flux from these central stars.

In a recent paper by Zhang and Kwok (1992) the age and core mass of the central
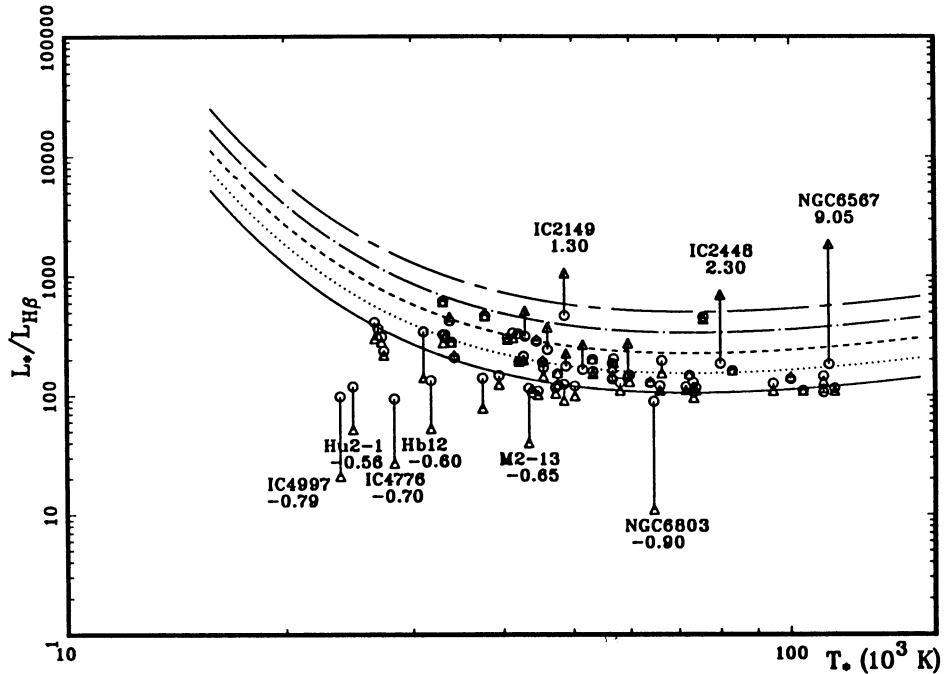
Fig. 2. $L_* / L_{H\beta}$ as a function of $T_*$. Solid, dotted, dashed, chain-dotted, and chain-dashed curves are for mean UV optical depths of 0, 0.5, 1., 1.5, and 2 respectively. Open circles and triangles are data points of $F_t/F_{H\beta}$ and $F_{BB}/F_{H\beta}$ respectively. Vertical lines connect the pairs of data points belonging to the same objects.

star have been derived from the distance- independent parameters for 302 galactic PN. If the ratio of $F_{IR}/F_t$ is plotted against the central star age ($t_*$), it appears that this ratio decreases with increasing age. This indicates that as a nebula ages, the dust tends to contribute less. This conclusion is confirmed by the theoretical modeling of the evolution of PN spectra (Volk 1992). It is conceivable that as the dust shell expands, the dust grains become cooler, and emit less far-ir radiation in the IRAS wavelength bands.

## 5. Conclusion

Significant progress has been made in our understanding of energy distribution of PN for a vastly wide wavelength coverage from UV to radio. It is expected further observations using the Space Telescope, ROSAT, ISO, and ground-based telescopes will fill many holes left in the current wavelength coverage. I would draw attention to near-ir surveys of the 2-MASS and DENIS projects. These deep surveys will provide us with unprecedented results and shed light on this less thoroughly explored wavelength range.

# References

Aaquist, O.B., and Kwok, S. 1990, A&AS 84, 229
Acker, A., Koppen, J., Stenholm, B., and Jasniewicz, G. 1989a, A&AS 80, 201
Acker, A., Koppen, J., Stenholm, B., and Raytchev, B. 1991, A&AS 89, 237
Acker, A., and Stenholm, B. 1987, The Messenger 48, 16
Acker, A., Stenholm, B., and Tylenda, R. 1989b, A&AS 77, 487
Aller, L.H., and Czyzak, S.J. 1979, Ap&SS 62, 397
Aller, L.H., and Czyzak, S.J. 1983, ApJS 51, 211

Bianchi, L., Recillas, E., and Grewing, M. 1989, in IAU Symp. No. 131, p.307
Boroson, T.A., and Leibert, J. 1989, ApJ 339, 844
Boggess, A., Freibelman, W.A., and McCracken, C.W. 1981, NASA Publ. 2171, 663
Brown, R.L., and Mathews, W.G. 1970, ApJ 160, 939
Clegg, R.E.S., and Middlemass, D. 1987, MNRAS 228, 779
Gacia-Lario, P., Manchado, A., Pottasch, S.R., Suso, J., Olling, R. 1990, A&AS 82, 497
Gathier, R., and Pottasch, S.R. 1989, A&A 209, 369
Heap, S.R., and Augensen, H.J. 1987, ApJ 313, 268
Henry, R.B.C., and Shipman, H.L. 1986, ApJ 311, 774
Husfeld, D., Kudritzki, R.P., Simon, K.P., and Clegg, R.E.S. 1984, A&A 134, 139
IRAS Point Source Catalog, vers. 2, 1988, Joint IRAS Science Working Group, Washington DC: GPO
IRAS Science Team: 1986, IRAs Catalog and Atlases, Atlas of Low Resolution Spectra, A&AS 65, 607
Jacoby, G.H., and Kaler, J.B. 1989, AJ 98, 1662
Kaler, J.B. 1976a, ApJ 210, 113
Kaler, J.B. 1976b, ApJS 31, 517
Kaler, J.B. 1978, ApJ 226, 947
Kaler, J.B., and Feibelman W.A. 1985, ApJ 297, 724
Kaler, J.B. 1989, IAU Symp. No. 131, p.229
Kaler, J.B., Shaw, R.A., Feibelman, W.A., Imhoff, C.L. 1991, PASP 103, 67
Kaler, J.B., Shaw, R.A., Kwitter, K.B. 1990, ApJ 359, 392
Kohoutek, L., and Martin, W. 1981, A&AS 44, 325
Kwok, S. 1982, ApJ 258, 280
Kwok, S., Hrivnak, B.J., and Milone, E.F. 1986, ApJ 303, 451
Manchado, A., Pottasch, S.R., Garcia-Lario, P., Esteban, C., Mampaso, A. 1989, A&A 214, 139
Marionni, P.A., and Harrington, J.P. 1981, NASA Publ. 2171, 633
Meatheringham, S.J., and Dopita, M.A. 1991, ApJS 75, 407
Mendez, R.H., Kudritzki, R.P., Herrero, A., Husfeld, D., and Groth, H.G. 1988, A&A 190, 113
Mendez, R.H., Kudritzki, R.P., Herrero, A., 1992, A&A in press
Monk, D.J., Barlow, M.J., Clegg, R.E.S. 1988, MNRAS 234, 583
Pottasch, S.R., Baud, B., Beintema, D., Emerson, J., Habing, H.J., and Haris, S. 1984, A&A 138, 10
Pottasch, S.R., Preite-Martinez, A., Olnon, F.M., Mo, J.E., and Kingma, S. 1986, A&A 161, 363
Preite-Martinez, A., and Persi, P. 1989, A&A 218, 264
Ratag, M.A., Pottasch, S.R., Zijlstra, A.A., Menzies, J. 1990, A&A 233, 181
Rudy, R.J., Cohen, R.D., Rossano, G.S., Erwin, P., Puetter, R.C., Lynch, D.L.K. 1991a, ApJ 380, 151
Rudy, R.J., Rossano, G.S., Erwin, P., Puetter, R.C. 1991b, ApJ 368, 468
Shaw, R.J., and Kaler, J.B. 1985, ApJ 295, 537
Shaw, R.J., and Kaler, J.B. 1989, ApJS 69, 495
Stasinska, G., Tylenda, R., Acker, A., Stenholm, B. 1991, A&A 247,173
Terzian, Y. 1991, in Asteroids to Quasars, ed. P.M. Lugger (Cambridge Univ. Press), p.105
Torres-Peimbert, S., and Peimbert, M. 1977, Rev. Mex. Astron. Astrof. 2, 181
Tylenda, R., Acker, A., Gleizes, F., and Stenholm, B. 1989, A&AS 77, 39
Tylenda, R., Acker, A., Stenholm, B. Gleizes, F., and Raytchev, B. 1991a, A&AS 89, 77
Tylenda, R., Stasinska, G., Acker, A., and Stenholm, B. 1991b, A&A 246, 221
van der Veen, W.E.C.J., Habing, H.J., Geballe, T.R. 1989, A&A 226, 108

Volk, K. 1992, ApJS 80, 247
Volk, K., and Cohen, M. 1990, AJ 100, 485
Webster, B.L. 1988, MNRAS 230, 477
Whitelock, P.A. 1985, MNRAS 221, 63
Zhang, C.Y., and Kwok, S. 1990, A&A 237, 479
Zhang, C.Y., and Kwok, S. 1991, A&A 250, 179
Zhang, C.Y., and Kwok, S. 1992, ApJ 385, 255
Zhang, C.Y., and Kwok, S. 1992, A&A in press
Zijlstra, A.A., Pottasch, S.R., and Bignell, R.C. 1989, A&AS 79, 3292